METABOLIC PROFILING OF POTENTIAL LUNG CANCER BIOMARKERS USING BRONCHOALVEOLAR LAVAGE FLUID AND THE INTEGRATED DIRECT INFUSION/ GAS CHROMATOGRAPHY MASS SPECTROMETRY PLATFORM

Belén Callejón-Leblic[a,b,c], Tamara García-Barrera[*a,b,c], Jesús Grávalos-Guzmán[d], Antonio Pereira-Vega[d], José Luis Gómez-Ariza[*a,b,c]

[a]Department of Chemistry, Faculty of Experimental Sciences. University of Huelva. Campus de El Carmen. 21007, Huelva. SPAIN; [b]International Agrofood Campus of Excellence International ceiA3. University of Huelva. SPAIN; [c]Research Center of Health and Environment (CYSMA). University of Huelva. Campus de El Carmen. 21007, Huelva. SPAIN; [d]Pneumonology Area of Juan Ramón Jiménez Hospital, Huelva, Spain

*Corresponding authors at:

Department of Chemistry. Faculty of Experimental Science. University of Huelva. Campus de El Carmen. 21007, Huelva. Tel.: +34959219968, fax: +34 959 219942, e-mail address: ariza@uhu.es (J.L. Gómez-Ariza)

Department of Chemistry. Faculty of Experimental Science. University of Huelva. Campus de El Carmen. 21007, Huelva. Tel.: +34959219962, fax: +34 959 219942, e-mail address: tamara@dqcm.uhu.es (T. García-Barrera)

Abstract

Lung cancer is one of the ten most common causes of death worldwide, so that the search for early diagnosis biomarkers is a very challenging task. Bronchoalveolar lavage fluid (BALF) provides information on cellular and biochemical epithelial surface of the lower respiratory tract constituents and no previous metabolomic studies have been performed with BALF samples from patients with lung cancer. Therefore, this fluid has been explored looking for new contributions in lung cancer metabolism. In this way, two complementary metabolomics techniques based on direct infusion high resolution mass spectrometry (DI-ESI-QTOF-MS) and gas chromatography mass spectrometry (GC-MS) have been applied to compare statistically differences between lung cancer (LC) and control (C) BALF samples, using partial least square discriminant analysis (PLS-DA) in order to find and identify potential biomarkers of the disease. A total of 42 altered metabolites were found in BALF from LC. The metabolic pathway analysis showed that glutamate and glutamine metabolism pathway was mainly altered by this disease. In addition, we assessed the biomarker specificity and sensitivity according to the area under the receiver operator characteristic (ROC) curves, indicating that glycerol and phosphoric acid were potential sensitive and specific biomarkers for lung cancer diagnosis and prognosis.

Biological Significance

The search for early diagnosis of lung cancer is a very challenging task because of the high mortality associated to this disease and its critical linkage to the initiation of treatment. Bronchoalveolar lavage fluid provides information on cellular and biochemical epithelial surface of the lower respiratory tract constituents and no previous metabolomic studies have been performed with BALF samples from patients with lung cancer. Since BALF is in close interaction with lung tissue it is a more representative sample of lung status than other peripheral biofluids as blood or urine studied in previous works. Therefore, this study represents an innovative contribution in this topic that complement previous investigations about lung cancer, opening up new possibilities for understanding the pathogenesis of this disease and the use of efficient biomarkers.

Keywords.- lung cancer; metabolomics; bronchoalveolar fluid; biomarkers; direct infusion mass spectrometry; gas chromatography mass spectrometry

1. Introduction

Lung cancer (LC) is one of the most common cause of cancer-related deaths in the world provoking more than 1.3 million deaths each year [1,2]. It is an unspecific disease difficult to distinguish from other lung disorders [2], which generally leads to late diagnosis after a symptomatic stage with averaged survival period no longer than five-year in about the 15% of cases [3–5]. However, the early disease diagnosis increases this rate up to 85 % [2,6–8].

Metabolomics is a powerful tool for untargeted simultaneous analysis of a large number of metabolites to provide the corresponding "metabolomics fingerprint", which allows tracing the concentration and fluxes of metabolites and their identification, to deepen the pathology of diseases, biomarkers discovery and drug development [9]. Consequently, metabolomics has been used for LC biomarkers searching in different biological fluids and tissues applying NMR [10] and MS methods. These later include, generally, the couplings HPLC-MS (high performance liquid chromatography mass spectrometry), LC/MS/MS (liquid chromatography with tandem mass spectrometry) [10], liquid chromatography with high resolution mass spectrometry (HPLC-Q-TOF-MS) [12], CE-MS (capillary electrophoresis mass spectrometry) [11], and gas chromatography mass spectrometry (GC-MS) [13], in order to reduce the complexity of mass spectra, avoiding isobaric interferences and ion suppression of very low abundant

metabolites. However, separation devices increase the time of analysis and introduce inter-sample variability, reducing the metabolic information due to the analytical bias and "filter effect" represented by the separation step. For these reasons, direct infusion mass spectrometry (DIMS) without any previous separation step has also been proposed for this purpose [4,14]. This technique has several advantages as high-throughput screening capability, since it avoids the conventional time-resolved introduction of metabolites into the MS after the chromatographic separation, improving the analysis rapidity and non-targeted metabolite coverage [14–16], since there is not exclusion of compounds caused by the separation device. Limitations in identification of metabolites by DIMS due to isobaric interferences from complex matrices as serum are overcome with high resolution and high-mass accuracy analyzers, such as time-of-flight (TOF), Fourier transform ion cyclotron resonance (FTICR) [17] and Orbitrap [18] systems.

A number of biological fluids and tissue biopsy have been reported for LC diagnosis, as serum [3,19], plasma [4,20], urine [21–23], saliva [24], and lung tissues [25,26], but there are not antecedents about the use of bronchoalveolar lavage fluid (BALF) for this purpose. BALF is obtained during the exploratory study of patients with lung diseases and provides constituents information on cellular and biochemical epithelial surface of the lower respiratory tract through instillation and later aspiration of liquid in one or more lung segments. It is estimated that BALF samples take a million cells (1% of the lung surface) to yield about 1 ml of pulmonary secretions in the actual total recovered liquid [27]. Because of BALF is in close interaction with lung tissue is a more representative sample of lung status than other peripheral biofluids as blood or urine.

Previous metabolomic studies based on BALF samples consider different lung diseases, such as asthma, [28,29] respiratory distress syndrome [30,31], immunodeficiency virus type 1 (IHV-1) [32] or cystic fibrosis [33], but never has been applied to LC patients.

The present work explores for the first time the combined application of direct infusion electrospray ionization triple quadrupole time-of-flight mass spectrometry (DI-ESI-QqQ-TOF-MS) and GC-MS to the metabolomic study of BALF samples from lung cancer and other pulmonary (non-cancer) patients. It has been applied a metabolomic platform based on mass spectrometry techniques combining direct infusion triple quadrupole time-of-flight mass spectrometry with an ionization electrospray source (DI-ESI-QTOF-MS) and gas chromatography mass spectrometry (GC-MS), for a total of 55 BALF samples (24 LC and 31 control subjects (CS)). In addition, statistical methods (partial least square discriminant analysis (PLS-

DA)) was applied to establish discriminations between groups and identify the altered metabolites related to this, which could be used as potential biomarkers for early diagnosis of LC.

2. Material and methods

2.1. Sample collection

BALF samples were collected from 24 LC and 31 control patients (C), the later without lung cancer, at the Pneumonology Area of Juan Ramón Jiménez Hospital (Huelva, Spain) from July 2011 to October 2013. The BALF samples were divided into aliquots of 1 ml in Eppendorf tubes and stored at -80 ºC until analysis. Sex and ages data of LC and C patients are shown in Table 1, and the diseases suffered by C patients in Table 2.

Table 1. Sex and age data of lung cancer patients and controls

	LC (n=24)	C (n=31)
Sex (male/female)	16/8	23/8
Age (years)	66±11	56±13

Table 2. Lung diseases of 31 control patients

Pulmonary disease in C	C (n=31)
Lung contusion	1
Interstitial lung disease (ILD)	16
Pulmonary emphysema	3
Hemoptysis	5
Infectious BQ	4
Interstitial edema	2

The study was performed in accordance with the principles contained in the Declaration of Helsinki and approved by the Ethical Committee of University of Huelva.

2.2. Reagents

All the solvents used were of HPLC-grade. Methanol, chloroform and pyridine were purchased from Aldrich (Steinheim, Germany). Formic acid was supplied by Merck (Darmstadt, Germany), and derivatizing agents, namely methoxylamine hydrochloride and N-methyl-N-(trimethylsilyl) trifluoroacetamide (MSTFA) were also obtained from Aldrich. Water was purified with a Milli-Q Gradient system (Millipore, Watford, UK).

2.3. Sample preparation

BALF samples were differently treated depending on the metabolomic technique applied. In the case of DI-ESI-QTOF-MS, we used the method proposed by Charles R. Evans et al., [30] based on the addition of 400 µl of 9:1 (v/v) methanol/chloroform mixture to 100 µl of BALF. The mixture was vortexed followed by centrifugation at 15000 g for 10 min, and the supernatant was directly infused into the MS spectrometer for analysis by electrospray mass spectrometry; 0.1% formic acid was added to the extracts if positive ionization mode of analysis is used.

For GC-MS, 500 µl of BALF samples were pre-concentrated using a speed vacuum system (SpeedVacTM Thermo Scientific) during 1h at 45 ºC, and reconstituted with the derivatizing agents. For protection of carbonyl groups by methoxymation, dried extracts were redissolved in 50 µl of 20 mg mL^{-1} methoxyamine in pyridine, and after briefly vortexing were incubated at 80◦C for 15 min in a water bath. Subsequently, silylation was performed by adding 50 µl of MSTFA and incubation at 80◦C for 15 min. Finally, extracts were centrifuged at 4000 rpm for 5 min and the supernatant collected for analysis.

2.4. Quality controls

A total of ten Quality control samples (QCs) were prepared by pooling equal volumes of all samples studied, which were treated with the sample procedure and analyzed for both DI-ESI-QTOF and GC-MS.

2.5. DI-ESI-QTOF-MS and GC-MS analysis

The DI-ESI-QTOF-MS experiments were performed in a QSTAR XL Hybrid system (Applied Biosystems, Foster City, CA, USA) using the electrospray (ESI) source. The samples were introduced into the mass spectrometer at 5 µl/min flow rate using an integrated apparatus pump and a 1000 µl volume Hamilton syringe. Data were obtained in both positive and negative ionization modes, acquiring full scan spectra for 0.2 minutes in the m/z range 50-1100 uma with 1.005 seconds of scan time. The parameters of the Q-TOF system were optimized to obtain the higher sensitivity with minimal fragmentation of molecular ions. In positive mode, the ion spray voltage (IS) was set at 3300 V, and high-purity nitrogen was used as curtain and nebulizer gas at flow rates about 1.13 l/min and 1.56 l/min, respectively. The source temperature was fixed at 60ºC, with a declustering potential (DP) of 60 V and a focusing potential (FP) of 250 V. The ion energy (IE) was fixed at 2.0 V with a channel electron multiplier (CEM) of 2150 V. To acquire MS/MS spectra, nitrogen was used as collision gas.

154

155 Gas chromatographic analysis was performed in a Trace GC ULTRA gas chromatograph coupled to an
156 ion trap mass spectrometer detector ITQ900 (Thermo Fisher Scientific), using a Factor Four capillary
157 column VF-5MS 30 m × 0.25 mm ID, with 0.25 µm of film thickness (Varian). The GC column
158 temperature was set to 100ºC for 0.5 min, and programmed to reach 320ºC at a rate of 15ºC per minute.
159 Finally, this temperature was maintained for other 7 min, being the total time of analysis 22.17 min. The
160 injector temperature was kept at 280ºC, and helium was used as carrier gas at a constant flow rate of 1 ml
161 min^{-1}. For mass spectrometry detection, ionization was carried out by electronic impact (EI) with a
162 voltage of 70 eV, by full scan mode in the m/z range 35–650, with anion source temperature of 200ºC.
163 For analysis, 1 µl of sample was injected in splitless mode.

164

165 **2.6. Data processing**

166 Mass data from DI-ESI-QTOF-MS were extracted directly from QSTAR XLSTAR XL Hybrid system
167 software (Applied Biosystems, Foster City, CA, USA) in .wif files to be exported to Markerview™
168 software (Applied Biosystems) that filtered the mass spectrometric data in order to reduce m/z data and
169 peaks intensities for two-two dimensional matrices construction. For this purpose a filter intensity of 10
170 counts and a t-test were used to eliminate non-significant variables from the dataset. In addition, the
171 results were submitted to normalization using total area sum in order to correct possible instrumental
172 drifts.

173 In the case of GC-MS, raw data was processed following the pipeline described by Katajamaa and Oresic
174 [34], which proceeds through multiple stages including feature detection, alignment of peaks and
175 normalization. For this purpose was used the freely available XCMS software, included in the R platform
176 (http://www.r-project.org). Files were converted into net CDF using the Thermo File Converter tool
177 (Thermo Fisher Scientific) and subsequently, data were extracted using the matched filter method. This
178 algorithm slices data into extracted ion chromatograms (XIC) on a fixed step size, and then each slice is
179 filtered with matched filtration using a second-derivative Gaussian as the model peak shape [35]. The
180 XCMS parameters were optimized according to the characteristics of datasets obtained in order to extract
181 the maximum information as possible. Finally, the settings applied for GC-MS data were S/N threshold 2,
182 full width at half-maximum (fwhm) 3, and width of the m/z range 0.1 (step parameter). After peak
183 extraction, grouping and retention time correction of peaks (alignment) was accomplished in three

iterative cycles with descending bandwidth (bw) from 5 to 1 s. Then, imputation of missing values was performed by returning to the raw spectral data and integrating the areas of the missing peaks which are below the applied signal-to-noise ratio threshold, using the fill Peaks algorithm. For data normalization, the locally weighted scatter plot smoothing (LOESS) normalization method was used, which adjusts the local median of log fold changes of peak intensities between samples in the data set to be approximately zero across the whole peak intensity range [36]. The preprocessed data were then exported as a .csv file for further data analysis by t-test to eliminate non-significant features following by multivariate procedures.

2.7. Statistical Analysis

Both DI-ESI-QTOF-MS and GC-MS data were processed with SIMCA-P™ software (version 11.5, published by UMetrics AB, Umeå, Sweden), to perform partial least squares discriminant analysis (PLS-DA) in order to discriminate between the groups of the study (LC vs C). Before performing statistical analysis, data was submitted to Pareto scaling, for reducing the relative importance of larger values, and logarithmic transformation, in order to approximate to a normal distribution [37]. Performance of models was assessed by the R2 and Q2 values, provided by the software (indicative of class separation and predictive power of the model, respectively). Finally, metabolites responsible for discrimination were selected according to the Variable Importance in the Projection, or VIP (a weighted sum of squares of the PLS weight, which indicates the importance of the variable in the model), considering only variables with VIP values higher than 1, indicative of significant differences among groups. In the case of DI-ESI-QTOF-MS, potential biomarkers were identified using fragmentation analysis by MS/MS and matching the resulting fragmentation spectra with metabolomics data bases like HMDB (http://www.hmdb.ca/), o METLIN (hhtp://metlin.scripps.edu/). In the case of GC-MS, the NIST Mass Spectral Library (version 08) was used to identify the altered metabolites, considering only those variables with a Similarity Index (SI) greater than 70%. On the other hand statistical significance was analyzed using one-way ANOVA followed by multiple tests correction with the Tukey test (Statistica 8.0, StafSoft), using a level of probability of 0.05 as criterion for significance.

2.8. Metabolic pathway analysis

Metabolic pathway analysis was performed to identify the affected pathways on the basis of altered metabolites. The Metaboanalyst 3.0 web tool (http://www.metaboanalyst.ca/) was used for this purpose, which conducts pathway analysis through pathway enrichment analysis and pathway topological analysis [38]. The "Homo sapiens" library was selected using the default "Hypergeometric Test" and "Relative-Betweenness Centrality" algorithms for pathway enrichment analysis and pathway topological analysis, respectively. In order to identify the most relevant pathways, the impact-value threshold calculated from pathway topology analysis was set at 0.1.

2.9. Potential lung cancer biomarkers from BALF

We assessed the potential biomarker specificity and sensitivity according to the area under the curve of the receiver operator characteristic (ROC), which could be used to distinguish patients with lung cancer from control subjects. The analysis was applied to the resulting altered metabolites in LC detected from both metabolomics techniques (DI-ESI-QTOF and GC-MS) using the Metaboanalyst 3.0 (http://www.metaboanalyst.ca/) software. Resulting data was carried out by logarithmic transformation and Pareto scaling.

3. Results

The BALF extracts from LC and C patients were analyzed using the two complementary metabolomic techniques, DI-ESI-Q-TOF-MS and GC-MS, the number of final features used for PLS-DA was 1352 and 1021, respectively. Typical mass spectra from LC and C cases are shown in Fig. 1(a) and (b), respectively.

The mass spectra data were used to construct the PLS-DA models which showed a good statistical classification between LC and C samples (Fig. 2). The quality of the model was evaluated by the relevant performance statistics of R2Y=0.966 and the predictive parameter Q2= 0.71, suggesting that the model was valid and highly predictive. It can be observed a good clustering in quality control samples (Fig. 2), indicative of results stability during analyses without significant outliers.

Metabolites responsible for the discrimination between LC and C patients were selected according VIP> 1, resulting in 24 altered metabolites in LC patients (Table 3). Potential biomarkers were identified

matching the experimental accurate mass and tandem mass spectra (MS/MS) with those shown in metabolomic databases (HMDB and METLIN), and then confirmed with commercial standards when available. Aminoacids, carnitines, lysophospholipids (lysophosphocholines (LPC) and lysophosphosphingosines (LPS)), phospholipids (phosphocholines (PC), phosphoethanolamines (PE) and phosphoethanolamines plasmalogens (PPE)) were altered in LC. In addition, the Table 3 collects the statistical significance of metabolites analyzed using one-way ANOVA followed by Tukey test. Finally, AUC values from ROC curves analysis are also shown in Table 3.

Table 3. Altered metabolites in LC samples detected with DI-ESI-QTOF-MS

Metabolite	m/z	Adduct	VIP	Sense of alteration	Fold change	*p* value	AUC
Urea	61.04	$[M+H^+]$	1.30	↓	0.74	0.048	0.54
Choline *	104.11	$[M+H^+]$	2.41	↓	0.68	0.014	0.78
L-Serine	106.05	$[M+H^+]$	1.31	↓	0.78	0.044	0.53
L-Valine	118.09	$[M+H^+]$	1.87	↓	0.57	0.040	0.66
PyroGlutamate	130.06	$[M+H^+]$	1.01	↓	0.83	0.042	0.57
Creatine	132.08	$[M+H^+]$	1.53	↓	0.76	0.032	0.60
Adenine *	136.08	$[M+H^+]$	1.27	↑	1.92	0.043	0.82
Acetylcholine	146.12	$[M+H^+]$	1.67	↓	0.61	0.027	0.57
L-Glutamate	148.07	$[M+H^+]$	1.58	↓	0.84	0.019	0.51
Carnitine *	162.11	$[M+H^+]$	2.67	↓	0.92	0.023	0.87
L-Arginine	175.11	$[M+H^+]$	1.43	↓	0.80	0.036	0.53
Phosphocholine	184.10	$[M+H^+]$	2.09	↑	1.48	0.046	0.67
Acetylcarnitine	204.28	$[M+H^+]$	1.71	↓	0.71	0.011	0.71
Glycerophosphocholine	296.07	$[M+K^+]$	1.14	↓	0.70	0.019	0.52
LPC(18:2)	520.34	$[M+H^+]$	1.10	↓	0.86	0.024	0.5
LPS(18:0)	526.37	$[M+H^+]$	1.63	↓	0.72	0.001	0.58
LPC(22:5)	570.36	$[M+H^+]$	1.60	↓	0.68	0.038	0.61
PE(16:0/18:0)	742.50	$[M+H^+]$	1.04	↓	0.90	0.023	0.59
PE(18:1/18:0)	746.50	$[M+H^+]$	1.36	↓	0.88	0.024	0.59
PE(18:0/18:0)	748.52	$[M+H^+]$	1.64	↓	0.85	0.006	0.56
PPE(18:1/20:4)	750.52	$[M+H^+]$	1.41	↓	0.86	0.028	0.55
PPE(18:0/20:4)	752.52	$[M+H^+]$	1.24	↓	0.86	0.047	0.52
PC(16:0/16:0)	756.56	$[M+Na^+]$	1.69	↓	0.60	0.047	0.56
PC(18:1/18:1)	808.55	$[M+Na^+]$	1.14	↓	0.80	0.041	0.51

*Metabolites with AUC> 0.75

Typical GC-MS chromatograms of BALF samples from LC and C patients are displayed in Fig. 3(a) and (b), respectively. The PLS-DA score plots from GC-MS data are shown in Fig 4 exhibiting a statistic performance of R^2Y=0.992 and the predictive parameter Q^2= 0.763. In addition, statistical significance was analyzed using one-way ANOVA followed by Tukey test (Statistica 8.0, StafSoft). On the other hand, AUC values of ROC curves analysis are also shown in Table 4. A total of 18 altered metabolites (Table 4) were identified in LC using the NIST Mass Spectral Library (version 08).

Table 4. Altered metabolites in LC BALF samples detected with GC-MS

Metabolite	Rt (min)	VIP	Sense of alteration	Fold change	*p* values	AUC
Lactic acid	2.87	1.96	↓	0.62	0.012	0.65
Acetic acid	3.38	1.93	↑	1.71	0.047	0.52
Glycerol *	4.28	2.18	↓	0.59	0.004	0.88
L-Glycine	4.63	1.49	↓	0.6	0.017	0.74
L-Aspartate	6.35	1.35	↓	0.48	0.047	0.74
L-Proline	6.45	1.01	↓	0.68	0.042	0.63
L-Glutamine	7.13	1.44	↓	0.50	0.033	0.66
Benzoic acid	7.267	1.01	↓	0.21	0.048	0.52
Fructose	7.57	1.66	↓	0.58	0.017	0.60
Phosphoric acid*	8.35	2.12	↓	0.42	0.047	0.79
Isocitric acid	8.57	1.67	↓	0.53	0.023	0.57
Inosytol	8.87	1.17	↓	0.63	0.028	0.58
Galactose	9.08	2.1	↓	0.63	0.043	0.68
Palmitic acid	10.18	2.11	↑	1.37	0.008	0.69
Stearic acid	11.38	1.88	↑	1.36	0.022	0.64
Inosine	13.13	1.02	↓	0.36	0.038	0.63
Oleic acid	13.7	1.45	↓	0.78	0.023	0.54
Cholesterol	16.13	1.55	↓	0.47	0.019	0.72

*Metabolites with AUC> 0.75

Subsequently, altered metabolic pathways associated with the expression of metabolites in LC were identified using the pathway analysis tool from "Metaboanalyst 3.0". A total of 41 metabolic routes have been altered in LC, which can be observed in Fig. 5, each dot represents a metabolic pathway and its size

indicates the impact of pathways in response to LC. Perturbations in the metabolism of glycerophospholipid, D-glutamine and D-glutamate, and glycine, serine and threonine have been observed, being the most altered pathways in LC according to the corresponding p and Impact values. The Fig. 6 shows a summary chart of the interconnected metabolic pathways related to altered metabolites in LC.

The values of AUC, obtained from the ROC curves, are shown in Table 3 and 4, revealing the altered metabolites clinically significant, since ROC curves with an AUC ≤ 0.75 are not considered. In this way, only five ROCs curves with AUCs values higher than 0.75 (Fig. 7) have been selected, and the corresponding metabolites related to them: carnitine, adenine, choline, glycerol and phosphoric acid can be considered as potential biomarkers of LC.

4. Discussion

The application for the first time of complementary metabolomic techniques based on DI-ESI-QTOF-MS and GC-MS to BALF samples, from lung cancer patients (24 cases) and pulmonary disease patients without cancer (31 cases), allowed to find 24 altered metabolites using DI-ESI-QTOF-MS and 18 by GC-MS analysis. The comparative study of metabolites identified with both metabolic platforms reveals the absence of matched altered metabolites that demonstrate the complementary character of both approaches and the more comprehensive metabolomic understanding provided in relation to lung cancer onset. On the other hand, comparison of results obtained in the present study based on BALF and those from serum of LC patients, this latter based on the results published by Hori et al [7], reveals an increase of altered metabolites in serum from LC patients (57 metabolites) against those from BALF (19 metabolites). Nevertheless, only four metabolites present alterations in both fluids, i.e., lactic acid, L-glycine, L-proline and phosphoric acid, although the change tendency is not the same in the case of lactic acid, L-glycine and L-proline whose levels decreases in BALF and increases in serum. However, phosphoric acid levels decreases in both fluids from LC patients with respect to controls. This fact reflects the interest of metabolomic studies of lung cancer patients based on BALF, with a more direct interaction with the damaged tissue, regarding to those from conventional peripheral serum samples.

Alterations in amino acids

The levels of several amino-acids suffered changes in BALF samples from lung cancer patients: L-glycine, L-valine, L-proline, L-serine, L-arginine, L-glutamate, L-aspartate, L-pyroglutamate and L-glutamine, which show clear reduction of levels (Tables 3 and 4) in accordance with previous studies on lung cancer cells [20,39–43]. This may be a consequence of both malnutrition suffering cancer patients as consequence of tumor-bearing state and the increase of amino acid demand caused by tumor itself growth [41]. Glutamine plays a significant role in cancer cell growth, protein translation, anaplerosis and macromolecule synthesis [44], since it is involved in purine and pyrimidine synthesis with glycine and aspartate. In addition glutamine/glutamate participate in the Glutamine-Glutamate metabolism, one of the most altered metabolic pathways in our study (Fig. 5), and with arginine also participate in urea cycle and consequently in the nitrogen metabolism. Pyroglutamate is a cyclic amino acid found at the N termini of some proteins and biological peptides and its formation occurs through the rearrangement of the originally synthesized glutamate or glutamine residues at this position [45]. On the other hand, cancer growth requires serine for membrane lipid component synthesis [41] and participates with L-valine and L-glycine in succynil-Coa synthesis, a basic component of Krebs cycle substratum. In the same way may be interpreted the decreasing of L-proline, a nonessential amino acid, formed from L-glutamate that participates in α-ketoglutarate synthesis, another substratum of Krebs cycle. All these metabolic perturbations reflect the well-known impact of cancer disease on energy cycle. Finally, glycine-serine-threonine metabolism is also one of the most altered metabolic pathways (Fig. 5).

Alterations in the levels of fatty acids and other organic acids

It has been found that levels of saturated fatty acids, such as stearic and palmitic acids, were increased in LC patients, whereas the unsaturated one oleic acid decreased, these changes can be associated to proliferating tumor cells that use long chain fatty acids for membrane assembly, lipid modifications of proteins and energy production [46].

Other organic acids as acetic, lactic, benzoic, phosphoric and isocitric acids were altered in LC. The levels of these compounds except acetic and lactic acids were lower in these patients. Lactic acid is the final end product of glycolysis, one of the metabolic routes affected in cancer because of the high consumption of glucose by cancer cell growth. In addition, many other studies in BALF samples suggested the increase of lactic acid because of lung inflammation [47] asthma [48,49] cystic fibrosis [33] or lung injuries [31], as a consequence of the low oxygen environment in lung that triggers anaerobic

metabolism and could result in increased level of lactate production [31]. On the other hand isocitric acid is related to the formation of α-ketoglutarate also involved in Krebs cycle, and phosphoric acid was one of the five metabolites that showed a high AUC value (AUC=0.79) becoming a potential biomarker for lung cancer.

Alteration of energy-related molecules

Adenine, which increased in LC patients, is other potential biomarker of this disease with an AUC value of 0.82. This purine base found in both DNA and RNA is a component of adenine nucleotides. Adenine forms adenosine, a nucleoside, when attached to ribose, and deoxyadenosine when attached to deoxyribose; it forms adenosine triphosphate (ATP), a nucleotide, when bound to three phosphate. The supply of ATP in human cells is provided by glycolysis and oxidative phosphorylation, this metabolite has an important role in cancerous processes since ATP supply is necessary for cancer cell survival and growth [50]. The degradation of these nucleotides by nucleotidases is the basis of the immune response or alternatively it may be used as a rapid energy source[51].

Carnitine and acetyl-carnitine decreased in LC patients, showing the former a high AUC value (AUC= 0.87). Both biomolecules are involved in β-oxidation of free fatty acids, which are transported across the inner mitochondrial membrane by carnitine and play an important role in several cellular processes such as phospholipid synthesis, protein kinase C activation (PKC), and β-oxidation [52–55]. The β-oxidation pathway is a dominant bioenergetics process in prostate cancer which increases fatty acid utilization to provide increased ATP levels; however, little is known about its role in lung cancer [56].

Creatine becomes phosphocreatine through a phosphorylation reaction catalyzed by the enzyme creatine kinase. In this process, an ATP molecule is also consumed. Phosphocreatine contributes to energy reserve that is quickly usable by skeletal muscle and other tissues. As a consequence, creatine decreased in lung cancer patients, in good agreement with Gazdar et al [57] who found that small-cell carcinomas of lung tumor specimens and continuous cultures also were characterized by high levels of creatine kinase suggesting a high activity of this enzyme and a high consumption of creatine to be converted to phosphocreatine, which provides energy to support cancer cells.

Glycerol is a three-carbon substance that forms the backbone of fatty acids in fats and, consequently, contributes to phospholipids biosynthesis. Glycerol can be converted to glucose by the liver and provides energy for cellular metabolism. Glycerol decreased in LC patients due to its rapid conversion to glucose, which increased in LC to sustain cancer growth [58]. On the other hand, fructose, galactose and turanose, implicated in carbohydrates metabolism decreased in LC suggesting also alterations in energy metabolism. Finally, cholesterol decreased in LC patients as has been reported by Chang AK et al., [59] that found lower levels of cholesterol in plasma of lung cancer patients than that in other type of cancer.

Alterations in the levels of lipids

Glycerophosphocholine, choline and phosphocholine are the last biomolecules involved in glycerophospholipid metabolism, one of the routes clearly altered in the pathway analysis (Figure 6, Table 4) as consequence of LC. Whereas glycerophosphocholine and choline decreased, phosphocholine increased in LC BALF samples suggesting the increased levels of apoptosis and necrosis. This result agrees with that from Yingrong et al.[3], who found increased levels of phosphocholine in the preoperative lung cancer patients comparing with healthy volunteers.

LPLs (LPCs, LPS) and PLs (PCs, PEs, PPEs) are altered in LC suggesting disturbances in glycerophospholipids metabolism in addition to be one of the three most altered pathways in LC according METPA analysis. Abnormalities in this metabolism, especially alteration in PC metabolism, are often found in cancer cells [60]. PL are major components of cell membranes, which are involved in the progression and metastasis of cancer when tumor cells undergo major morphological and molecular changes [61].

5. Conclusions

The application for the first time of a metabolomic platform based on mass spectrometry (DI-ESI-QTOF-MS and GC-MS) to bronchoalveolar lavage fluid from lung cancer patients has provided new information about the pathogeny of this disease. The study allows characterizing 42 altered metabolites involved in D-Glutamine/D-glutamate, glycine, serine/threonine and glycerophospholipid metabolisms, which are the most affected metabolic pathways in lung cancer. In addition, ROC curves analysis identified choline, adenine, carnitine, phosphoric acid and glycerol as potential biomarkers for lung cancer diagnosis with an

AUC value higher than 0.75. As a consequence, the use of BALF in lung cancer metabolomics is a good alternative that complement other more widely used peripheral fluids as serum, since the more direct interaction of BALF with tumor area will allow more reliable information on the pathogenic process.

Finally, the application of ROC curves used in this work is a very suitable method for potential biomarkers performance assessment. This is important because the final goal of biomarkers discovery is their translation to clinical practice [62]. In the present study, the five metabolites previously mentioned: choline, adenine, carnitine, phosphoric acid and glycerol could be recommended as multi-metabolite biomarker model to be translated to clinic trials based on target analysis supported by conventional analytical methodologies.

ACKNOWLEDGEMENTS

This work has been supported by the projects CTM2012-38720-C03-01 and CTM2015-67902-C2-1-P from the Spanish Ministry of Economy and Competitiveness and P12-FQM-0442 from the Regional Ministry of Economy, Innovation, Science and Employment (Andalusian Government, Spain). Neumosur scholarchip 8/2012 and Separ scholarship 124/2012. Belén Callejón Leblic thanks the Ministerio de Educación for a predoctoral scholarship FPU13/03615. Finally, authors are grateful to FEDER (European Community) for financial support.

REFERENCES

[1] R. Lozano, M. Naghavi, K. Foreman, S. Lim, K. Shibuya, V. Aboyans, et al., Global and regional mortality from 235 causes of death for 20 age groups in 1990 and 2010: a systematic analysis for the Global Burden of Disease Study 2010., Lancet. 380 (2012) 2095–128. doi:10.1016/S0140-6736(12)61728-0.

[2] A. Jemal, F. Bray, M.M. Center, J. Ferlay, E. Ward, D. Forman, Global cancer statistics., CA. Cancer J. Clin. 61 (2011) 69–90. doi:10.3322/caac.20107.

[3] Y. Chen, Z. Ma, A. Li, H. Li, B. Wang, J. Zhong, et al., Metabolomic profiling of human serum in lung cancer patients using liquid chromatography / hybrid quadrupole time-of-flight mass spectrometry and gas chromatography / mass spectrometry, (2015) 705–718. doi:10.1007/s00432-014-1846-5.

[4] P.G. Lokhov, O.N. Kharybin, A.I. Archakov, Diagnosis of lung cancer based on direct-infusion electrospray mass spectrometry of blood plasma metabolites, Int. J. Mass Spectrom. 309 (2012) 200–205. doi:10.1016/j.ijms.2011.10.002.

[5] J.R. Hocker, M.D. Peyton, M.R. Lerner, S.L. Mitchell, S.A. Lightfoot, T.J. Lander, et al., Serum discrimination of early-stage lung cancer patients using electrospray-ionization

mass spectrometry., Lung Cancer. 74 (2011) 206–11. doi:10.1016/j.lungcan.2011.03.014.

[6] A. Jemal, R. Siegel, E. Ward, Y. Hao, J. Xu, T. Murray, et al., Cancer statistics, 2008., CA. Cancer J. Clin. 58 (2008) 71–96. doi:10.3322/CA.2007.0010.

[7] S. Hori, S. Nishiumi, K. Kobayashi, M. Shinohara, Y. Hatakeyama, Y. Kotani, et al., A metabolomic approach to lung cancer., Lung Cancer. 74 (2011) 284–92. doi:10.1016/j.lungcan.2011.02.008.

[8] T. Wen, L. Gao, Z. Wen, C. Wu, C.S. Tan, W.Z. Toh, et al., Exploratory investigation of plasma metabolomics in human lung adenocarcinoma., Mol. Biosyst. 9 (2013) 2370–8. doi:10.1039/c3mb70138g.

[9] J.C. Lindon, E. Holmes, J.K. Nicholson, Metabonomics and its role in drug development and disease diagnosis., Expert Rev. Mol. Diagn. 4 (2004) 189–99. doi:10.1586/14737159.4.2.189.

[10] J.-H. Chen, B.M. Enloe, C.D. Fletcher, D.G. Cory, S. Singer, Biochemical Analysis Using High-Resolution Magic Angle Spinning NMR Spectroscopy Distinguishes Lipoma-Like Well-Differentiated Liposarcoma from Normal Fat, J. Am. Chem. Soc. 123 (2001) 9200–9201. doi:10.1021/ja016182u.

[11] R. Ramautar, A. Demirci, G.J. de Jong, Capillary electrophoresis in metabolomics, TrAC Trends Anal. Chem. 25 (2006) 455–466. doi:10.1016/j.trac.2006.02.004.

[12] F. Gosetti, E. Mazzucco, M.C. Gennaro, E. Marengo, Ultra high performance liquid chromatography tandem mass spectrometry determination and profiling of prohibited steroids in human biological matrices. A review., J. Chromatogr. B. Analyt. Technol. Biomed. Life Sci. 927 (2013) 22–36. doi:10.1016/j.jchromb.2012.12.003.

[13] Y. Niu, Y. Jiang, C. Xu, X. Wang, Y. Liu, H. Zhao, et al., Preliminary results of metabolite in serum and urine of lung cancer patients detected by metabolomics., Zhongguo Fei Ai Za Zhi. 15 (2012) 195–201. doi:10.3779/j.issn.1009-3419.2012.04.01.

[14] R. González-Domínguez, T. García-Barrera, J.L. Gómez-Ariza, Using direct infusion mass spectrometry for serum metabolomics in Alzheimer's disease., Anal. Bioanal. Chem. 406 (2014) 7137–48. doi:10.1007/s00216-014-8102-3.

[15] J. Draper, A.J. Lloyd, R. Goodacre, M. Beckmann, Flow infusion electrospray ionisation mass spectrometry for high throughput, non-targeted metabolite fingerprinting: a review, Metabolomics. 9 (2012) 4–29. doi:10.1007/s11306-012-0449-x.

[16] R. González-Domínguez, T. García-Barrera, J.L. Gómez-Ariza, Metabolomic study of lipids in serum for biomarker discovery in Alzheimer's disease using direct infusion mass spectrometry., J. Pharm. Biomed. Anal. 98 (2014) 321–6. doi:10.1016/j.jpba.2014.05.023.

[17] H. Takahashi, K. Kai, Y. Shinbo, K. Tanaka, D. Ohta, T. Oshima, et al., Metabolomics approach for determining growth-specific metabolites based on Fourier transform ion cyclotron resonance mass spectrometry., Anal. Bioanal. Chem. 391 (2008) 2769–82. doi:10.1007/s00216-008-2195-5.

[18] D. Favretto, E. Cosmi, E. Ragazzi, S. Visentin, M. Tucci, P. Fais, et al., Cord blood metabolomic profiling in intrauterine growth restriction., Anal. Bioanal. Chem. 402 (2012) 1109–21. doi:10.1007/s00216-011-5540-z.

[19] Y. Guo, X. Wang, L. Qiu, X. Qin, H. Liu, Y. Wang, et al., Probing gender-specific lipid metabolites and diagnostic biomarkers for lung cancer using Fourier transform ion cyclotron resonance mass spectrometry., Clin. Chim. Acta. 414 (2012) 135–41. doi:10.1016/j.cca.2012.08.010.

[20] J. Maeda, M. Higashiyama, A. Imaizumi, T. Nakayama, H. Yamamoto, T. Daimon, et al., Possibility of multivariate function composed of plasma amino acid profiles as a novel screening index for non-small cell lung cancer: a case control study., BMC Cancer. 10 (2010) 690. doi:10.1186/1471-2407-10-690.

[21] J. Carrola, C.M. Rocha, A.S. Barros, A.M. Gil, B.J. Goodfellow, I.M. Carreira, et al., Metabolic signatures of lung cancer in biofluids: NMR-based metabonomics of urine., J. Proteome Res. 10 (2011) 221–30. doi:10.1021/pr100899x.

[22] Y. Hanai, K. Shimono, K. Matsumura, A. Vachani, S. Albelda, K. Yamazaki, et al., Urinary volatile compounds as biomarkers for lung cancer., Biosci. Biotechnol. Biochem. 76 (2012) 679–84. doi:10.1271/bbb.110760.

[23] Q. Yang, X. Shi, Y. Wang, W. Wang, H. He, X. Lu, et al., Urinary metabonomic study of lung cancer by a fully automatic hyphenated hydrophilic interaction/RPLC-MS system., J. Sep. Sci. 33 (2010) 1495–503. doi:10.1002/jssc.200900798.

[24] S. Li, R. Wang, M. Zhang, L. Wang, S. Cheng, Proteomic analysis of non-small cell lung cancer tissue interstitial fluids., World J. Surg. Oncol. 11 (2013) 173. doi:10.1186/1477-7819-11-173.

[25] K.W. Jordan, C.B. Adkins, L. Su, E.F. Halpern, E.J. Mark, D.C. Christiani, et al., Comparison of squamous cell carcinoma and adenocarcinoma of the lung by metabolomic analysis of tissue-serum pairs., Lung Cancer. 68 (2010) 44–50. doi:10.1016/j.lungcan.2009.05.012.

[26] C.M. Rocha, A.S. Barros, A.M. Gil, B.J. Goodfellow, E. Humpfer, M. Spraul, et al., Metabolic profiling of human lung cancer tissue by 1H high resolution magic angle spinning (HRMAS) NMR spectroscopy., J. Proteome Res. 9 (2010) 319–32. doi:10.1021/pr9006574.

[27] A. Escribano Montaner, A. Moreno Galdó, Técnicas fibrobroncoscópicas especiales: lavado broncoalveolar, biopsia bronquial y biopsia transbronquial, An. Pediatría. 62 (2005) 352–366. doi:10.1157/13073249.

[28] W.E. Ho, Y.-J. Xu, C. Cheng, H.Y. Peh, S.R. Tannenbaum, W.S.F. Wong, et al., Metabolomics Reveals Inflammatory-Linked Pulmonary Metabolic Alterations in a Murine Model of House Dust Mite-Induced Allergic Asthma., J. Proteome Res. 13 (2014) 3771–3782. doi:10.1021/pr5003615.

[29] G. Haferburg, E. Kothe, Microbes and metals: interactions in the environment., J. Basic Microbiol. 47 (2007) 453–67. doi:10.1002/jobm.200700275.

[30] C.R. Evans, A. Karnovsky, M.A. Kovach, T.J. Standiford, C.F. Burant, K.A. Stringer, Untargeted LC-MS metabolomics of bronchoalveolar lavage fluid differentiates acute

514 respiratory distress syndrome from health., J. Proteome Res. 13 (2014) 640–9.
515 doi:10.1021/pr4007624.

516 [31] R.K. Rai, A. Azim, N. Sinha, J.N. Sahoo, C. Singh, A. Ahmed, et al., Metabolic
517 profiling in human lung injuries by high-resolution nuclear magnetic resonance
518 spectroscopy of bronchoalveolar lavage fluid (BALF), Metabolomics. 9 (2012) 667–676.
519 doi:10.1007/s11306-012-0472-y.

520 [32] Y. Park, D.M. Guidot, G.S. Martin, L.A. Brown, J. Lennox, D.P. Jones, Metabolomics
521 of Bronchoalveolar Lavage Differentiate Healthy HIV-1-Infected Subjects from
522 Controls, AIDS Res. Hum. Retroviruses. 30 (2014) 579–585.
523 doi:10.1089/aid.2013.0198.

524 [33] J.E. Wolak, C.R. Esther, T.M. O'Connell, Metabolomic analysis of bronchoalveolar
525 lavage fluid from cystic fibrosis patients., Biomarkers. 14 (2009) 55–60.
526 doi:10.1080/13547500802688194.

527 [34] M. Katajamaa, M. Oresic, Data processing for mass spectrometry-based metabolomics.,
528 J. Chromatogr. A. 1158 (2007) 318–28. doi:10.1016/j.chroma.2007.04.021.

529 [35] C.A. Smith, E.J. Want, G. O'Maille, R. Abagyan, G. Siuzdak, XCMS: processing mass
530 spectrometry data for metabolite profiling using nonlinear peak alignment, matching,
531 and identification., Anal. Chem. 78 (2006) 779–87. doi:10.1021/ac051437y.

532 [36] K.A. Veselkov, L.K. Vingara, P. Masson, S.L. Robinette, E. Want, J. V Li, et al.,
533 Optimized preprocessing of ultra-performance liquid chromatography/mass spectrometry
534 urinary metabolic profiles for improved information recovery., Anal. Chem. 83 (2011)
535 5864–72. doi:10.1021/ac201065j.

536 [37] R.A. van den Berg, H.C.J. Hoefsloot, J.A. Westerhuis, A.K. Smilde, M.J. van der Werf,
537 Centering, scaling, and transformations: improving the biological information content of
538 metabolomics data., BMC Genomics. 7 (2006) 142. doi:10.1186/1471-2164-7-142.

539 [38] J. Xia, D.S. Wishart, MetPA: a web-based metabolomics tool for pathway analysis and
540 visualization., Bioinformatics. 26 (2010) 2342–4. doi:10.1093/bioinformatics/btq418.

541 [39] A. Cascino, M. Muscaritoli, C. Cangiano, L. Conversano, A. Laviano, S. Ariemma, et
542 al., Plasma amino acid imbalance in patients with lung and breast cancer, Anticancer
543 Res. 15 (1995) 507–510. http://www.scopus.com/inward/record.url?eid=2-s2.0-
544 0029045178&partnerID=tZOtx3y1.

545 [40] A.M. Proenza, J. Oliver, A. Palou, P. Roca, Breast and lung cancer are associated with a
546 decrease in blood cell amino acid content, J. Nutr. Biochem. 14 (2003) 133–138.
547 doi:10.1016/S0955-2863(02)00225-5.

548 [41] H.-S. Lai, J.-C. Lee, P.-H. Lee, S.-T. Wang, W.-J. Chen, Plasma free amino acid profile
549 in cancer patients., Semin. Cancer Biol. 15 (2005) 267–76.
550 doi:10.1016/j.semcancer.2005.04.003.

551 [42] A. Kubota, M.M. Meguid, D.C. Hitch, Amino acid profiles correlate diagnostically with
552 organ site in three kinds of malignant tumors, Cancer. 69 (1992) 2343–2348.
553 http://www.scopus.com/inward/record.url?eid=2-s2.0-
554 0026529517&partnerID=tZOtx3y1.

[43] A.B. Naini, J.W.T. Dickerson, M.M. Brown, Preoperative and postoperative levels of plasma protein and amino acid in esophageal and lung cancer patients, Cancer. 62 (1988) 355–360. http://www.scopus.com/inward/record.url?eid=2-s2.0-0023928169&partnerID=tZOtx3y1.

[44] A.P.J. van den Heuvel, J. Jing, R.F. Wooster, K.E. Bachman, Analysis of glutamine dependency in non-small cell lung cancer: GLS1 splice variant GAC is essential for cancer cell growth., Cancer Biol. Ther. 13 (2012) 1185–94. doi:10.4161/cbt.21348.

[45] B. Blomback, Methods in Enzymology, C.Hirs, Academic Press, New York, USA, 1967.

[46] T. Mashima, H. Seimiya, T. Tsuruo, De novo fatty-acid synthesis and related pathways as molecular targets for cancer therapy., Br. J. Cancer. 100 (2009) 1369–72. doi:10.1038/sj.bjc.6605007.

[47] D. De Backer, J. Creteur, H. Zhang, M. Norrenberg, J.L. Vincent, Lactate production by the lungs in acute lung injury, Am. J. Respir. Crit. Care Med. 156 (1997) 1099–1104. http://www.scopus.com/inward/record.url?eid=2-s2.0-0030879973&partnerID=tZOtx3y1.

[48] W.E. Ho, Y.-J. Xu, F. Xu, C. Cheng, H.Y. Peh, S.R. Tannenbaum, et al., Metabolomics reveals altered metabolic pathways in experimental asthma., Am. J. Respir. Cell Mol. Biol. 48 (2013) 204–11. doi:10.1165/rcmb.2012-0246OC.

[49] W.E. Ho, Y.-J. Xu, F. Xu, C. Cheng, H.Y. Peh, S.-M. Huang, et al., Anti-malarial drug artesunate restores metabolic changes in experimental allergic asthma, Metabolomics. 11 (2014) 380–390. doi:10.1007/s11306-014-0699-x.

[50] R. Moreno-Sánchez, A. Marín-Hernández, E. Saavedra, J.P. Pardo, S.J. Ralph, S. Rodríguez-Enríquez, Who controls the ATP supply in cancer cells? Biochemistry lessons to understand cancer energy metabolism., Int. J. Biochem. Cell Biol. 50 (2014) 10–23. doi:10.1016/j.biocel.2014.01.025.

[51] S.S. Matsumoto, K.O. Raivio, J.E. Seegmiller, Adenine nucleotide degradation during energy depletion in human lymphoblasts. Adenosine accumulation and adenylate energy charge correlation, J. Biol. Chem. 254 (1979) 8956–8962. http://www.scopus.com/inward/record.url?eid=2-s2.0-0018664862&partnerID=tZOtx3y1.

[52] A. Guidotti, D.R. Konkel, B. Ebstein, M.G. Corda, B.C. Wise, H. Krutzsch, et al., Isolation, characterization, and purification to homogeneity of a rat brain protein (GABA-modulin)., Proc. Natl. Acad. Sci. 79 (1982) 6084–6088. doi:10.1073/pnas.79.19.6084.

[53] I.B. Mogensen, H. Schulenberg, H.O. Hansen, F. Spener, J. Knudsen, A novel acyl-CoA-binding protein from bovine liver. Effect on fatty acid synthesis, Biochem. J. 241 (1987) 189–192. http://www.scopus.com/inward/record.url?eid=2-s2.0-0023148729&partnerID=tZOtx3y1.

[54] Z. Chen, B. Agerberth, K. Gell, M. Andersson, V. Mutt, C.-G. Ostenson, et al., Isolation and Characterization of Porcine Diazepam-Binding Inhibitor, a Polypeptide Not Only of Cerebral Occurrence But Also Common in Intestinal Tissues and With Effects on Regulation of Insulin Release, Eur. J. Biochem. 174 (1988) 244–245. doi:10.1111/j.1432-1033.1988.tb14089.x.

598 [55] J.T. Rasmussen, N.J. Faergeman, K. Kristiansen, J. Knudsen, Acyl-CoA-binding protein
599 (ACBP) can mediate intermembrane acyl-CoA transport and donate acyl-CoA for β-
600 oxidation and glycerolipid synthesis, Biochem. J. 299 (1994) 165–170.
601 http://www.scopus.com/inward/record.url?eid=2-s2.0-
602 0028296147&partnerID=tZOtx3y1.

603 [56] Y. Liu, Fatty acid oxidation is a dominant bioenergetic pathway in prostate cancer.,
604 Prostate Cancer Prostatic Dis. 9 (2006) 230–4. doi:10.1038/sj.pcan.4500879.

605 [57] a. F. Gazdar, M.H. Zweig, D.N. Carney, a. C. Van Steirteghen, S.B. Baylin, J.D. Minna,
606 Levels of creatine kinase and its BB isoenzyme in lung cancer specimens and cultures,
607 Cancer Res. 41 (1981) 2773–2777.

608 [58] D. Heber, R.T. Chlebowski, D.E. Ishibashi, J.N. Herrold, J.B. Block, Abnormalities in
609 glucose and protein metabolism in noncachectic lung cancer patients, Cancer Res. 42
610 (1982) 4815–4819. http://www.scopus.com/inward/record.url?eid=2-s2.0-
611 0020426260&partnerID=tZOtx3y1.

612 [59] A.K. Chang, E. Barrettconnor, S. Edelstein, Low Plasma Cholesterol Predicts an
613 Increased Risk of Lung-Cancer in Elderly Women, Prev. Med. (Baltim). 24 (1995) 557–
614 562. doi:10.1006/pmed.1995.1089.

615 [60] K. Glunde, C. Jie, Z.M. Bhujwalla, Molecular causes of the aberrant choline
616 phospholipid metabolism in breast cancer., Cancer Res. 64 (2004) 4270–4276.
617 doi:10.1158/0008-5472.CAN-03-3829.

618 [61] K. Jelonek, M. Ros, M. Pietrowska, P. Widlak, Cancer biomarkers and mass
619 spectrometry-based analyses of phospholipids in body fluids, Clin. Lipidol. 8 (2013)
620 137–150. doi:10.2217/clp.12.79.

621 [62] M. Banez-Coronel, A. de Molina, A. Rodriguez-Gonzalez, J. Sarmentero, M. Ramos, M.
622 Garcia-Cabezas, et al., Choline Kinase Alpha Depletion Selectively Kills Tumoral Cells,
623 Curr. Cancer Drug Targets. 8 (2008) 709–719. doi:10.2174/156800908786733432.

624

625 **Figure captions**

626

627 **Figure 1.** (a) DI-ESI-MS spectrum of LC patients in positive ionization mode.

628 **Figure 1**. (b) DI-ESI-MS spectrum of C patients in positive ionization mode.

629 **Figure 2.** PLS-DA of DI-ESI-QTOF-MS data. Red points correspond to LC patients, black points to C
630 patients and grey points to the QCs.

631 **Figure 3.** (a) Typical GC-MS chromatogram of LC patients; (b) Typical GC-MS chromatogram of C
632 patients.

633 **Figure 4.** PLS-DA of GC-MS data. Red points correspond to LC patients, black points to C patients and
634 grey points to the QCs.

635 **Figure 5.** Overview of the most important metabolomic changes observed in BALF from LC patients. a:
636 D-Glutamine and D-glutamate metabolism, b: Glycine, serine and threonine metabolism, c:

637 Glycerophospholipid metabolism, d: Pyruvate metabolism, e: Alanine, aspartate and glutamate, f:
638 Galactose metabolism, g: Arginine and proline metabolism. P value is the p calculated from the
639 enrichment analysis and Impact is the pathway impact value calculated from pathway topology analysis.

640 **Figure 6.** Scheme of the most altered metabolic pathways in LC determined in the pathway analysis.

641 **Figure 7.** ROC curves with AUC values > 0.75 related to potential biomarkers of lung cancer. The red
642 point corresponds to the cutoff point of the curve where the metabolite is more sensitive and specific.

Figure 1a

Click here to download high resolution image

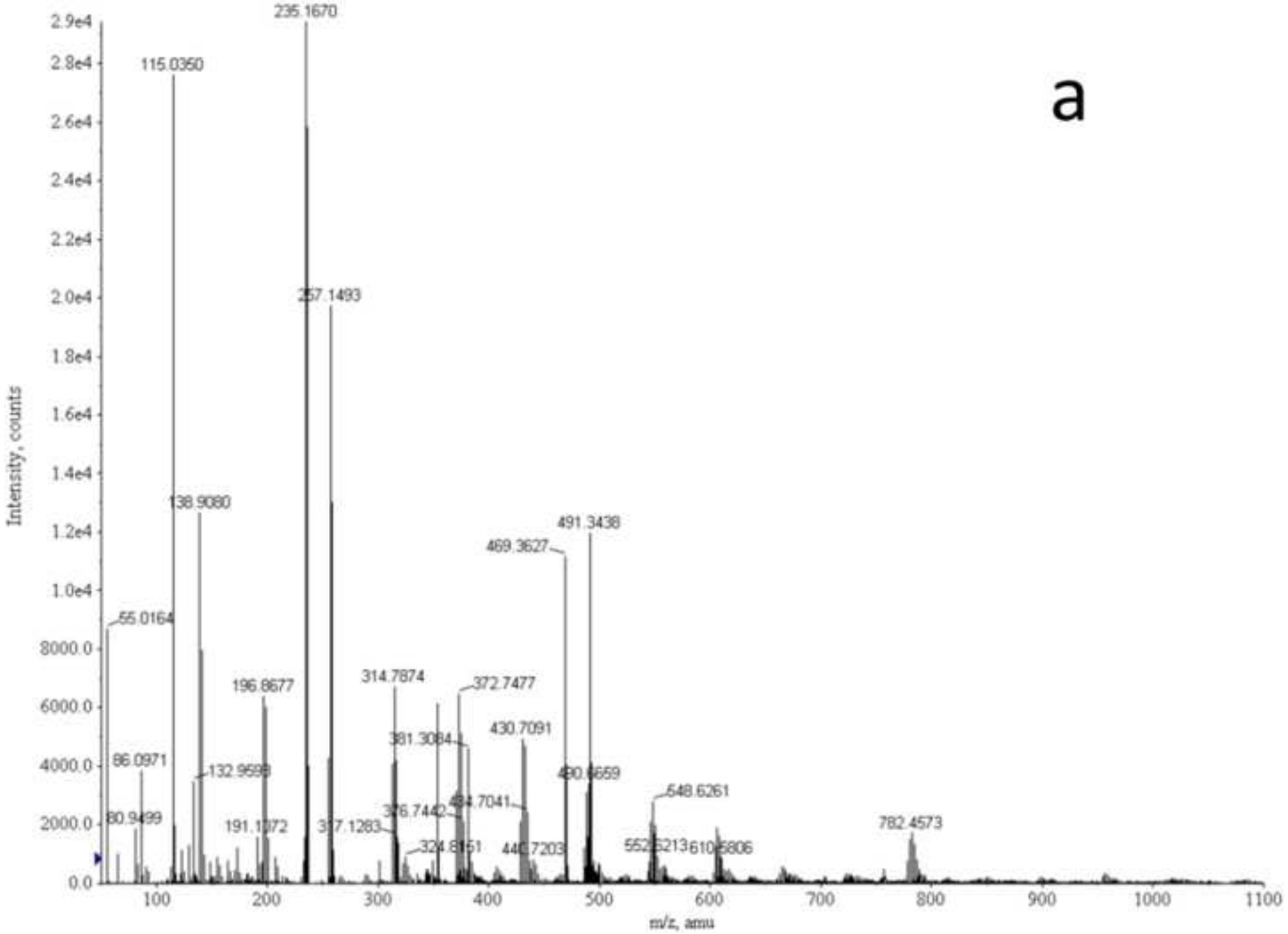

Figure 1b

Click here to download high resolution image

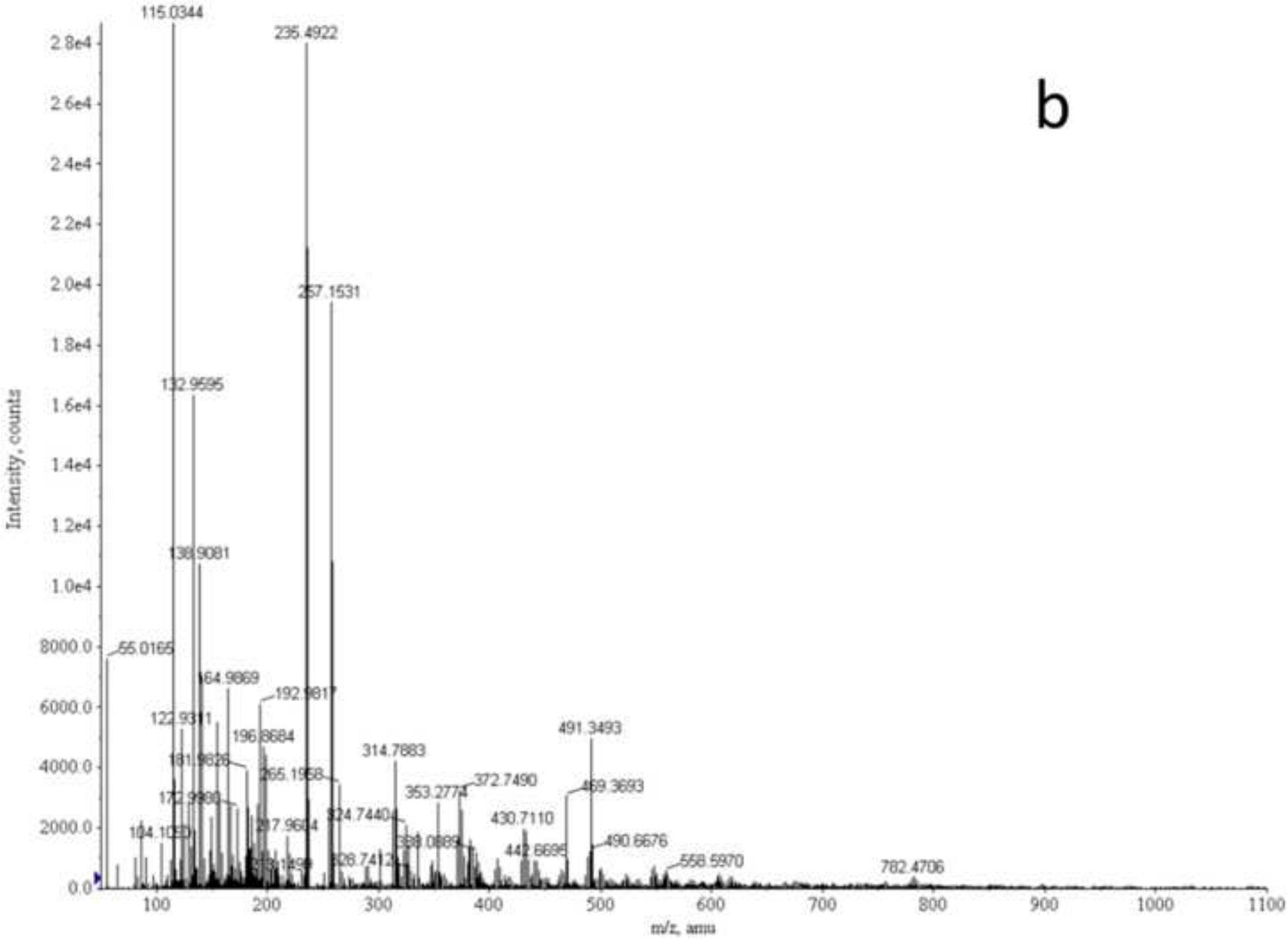

Figure 2

Click here to download high resolution image

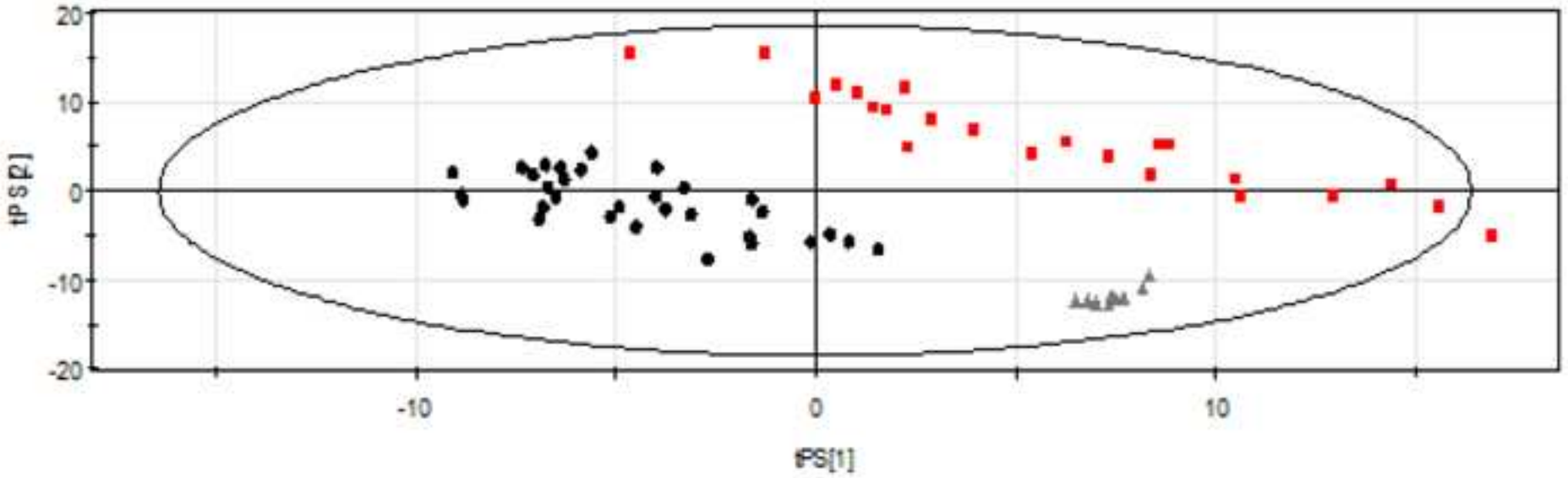

Figure 3

Click here to download high resolution image

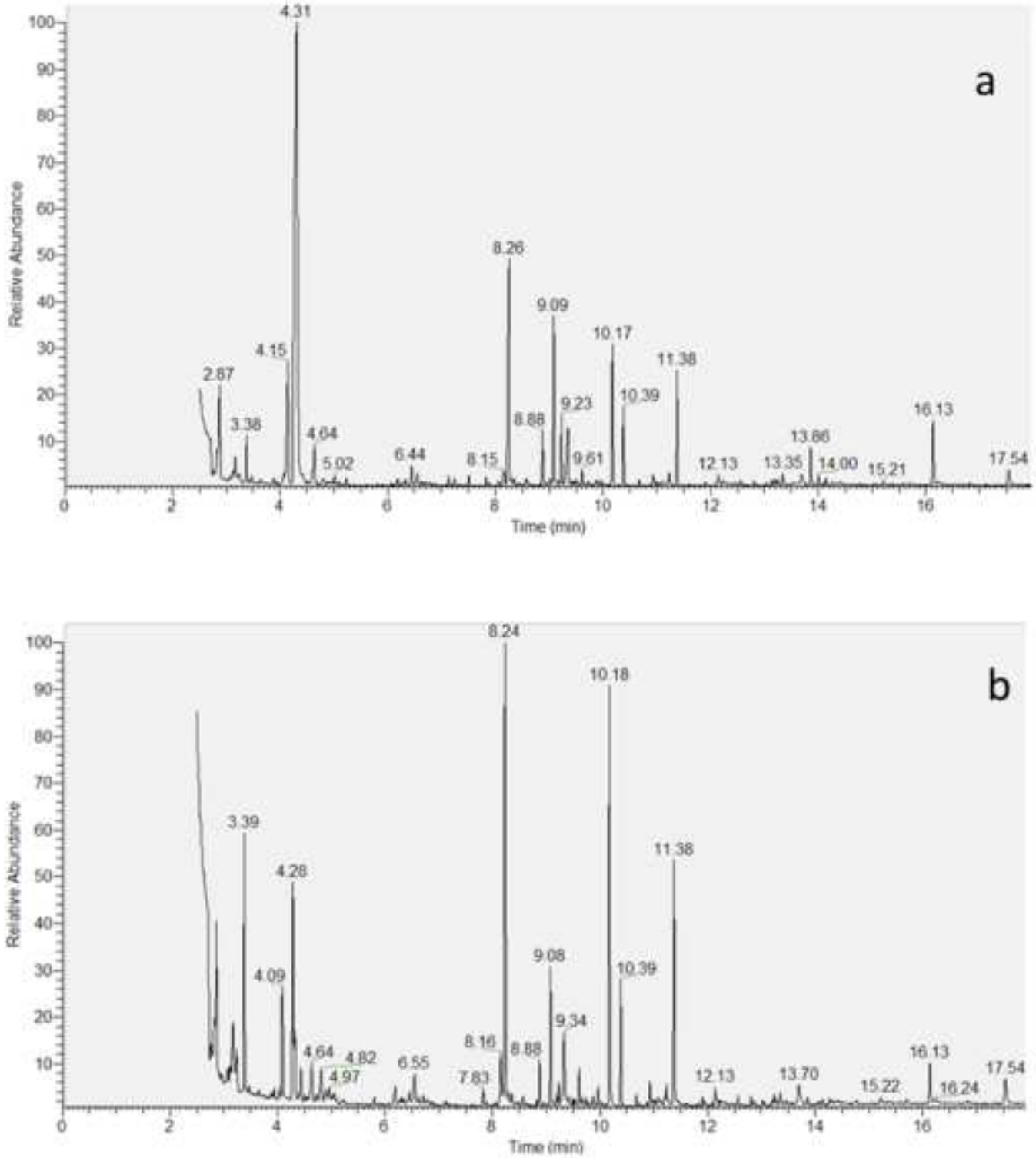

Figure 4

Click here to download high resolution image

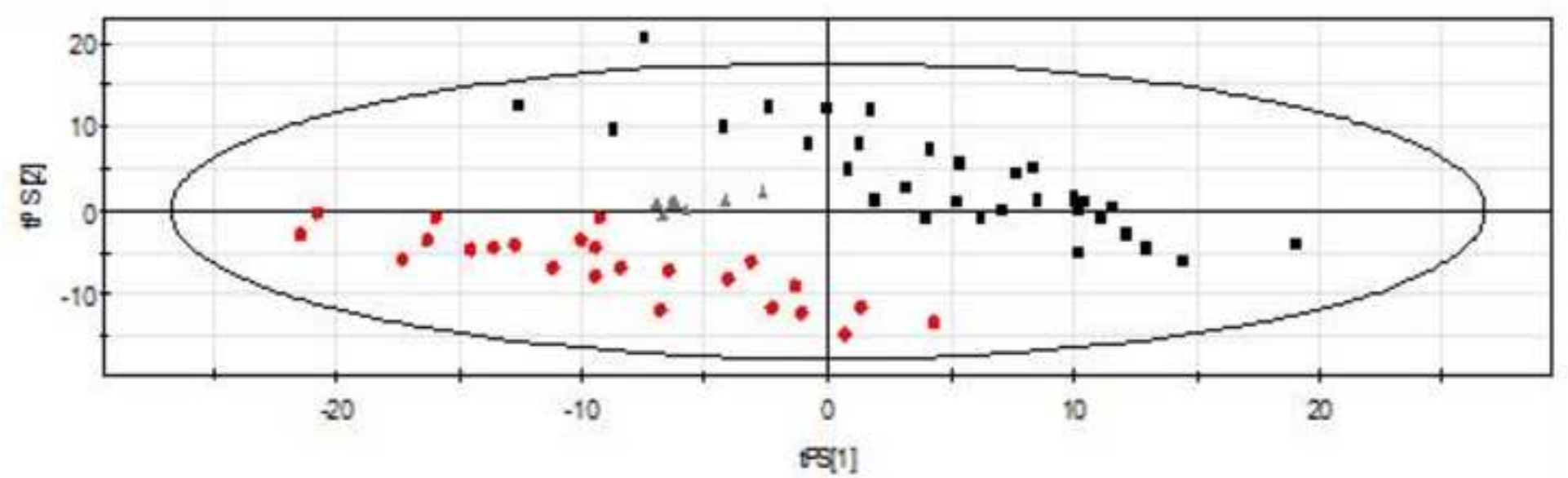

Figure 5

Click here to download high resolution image

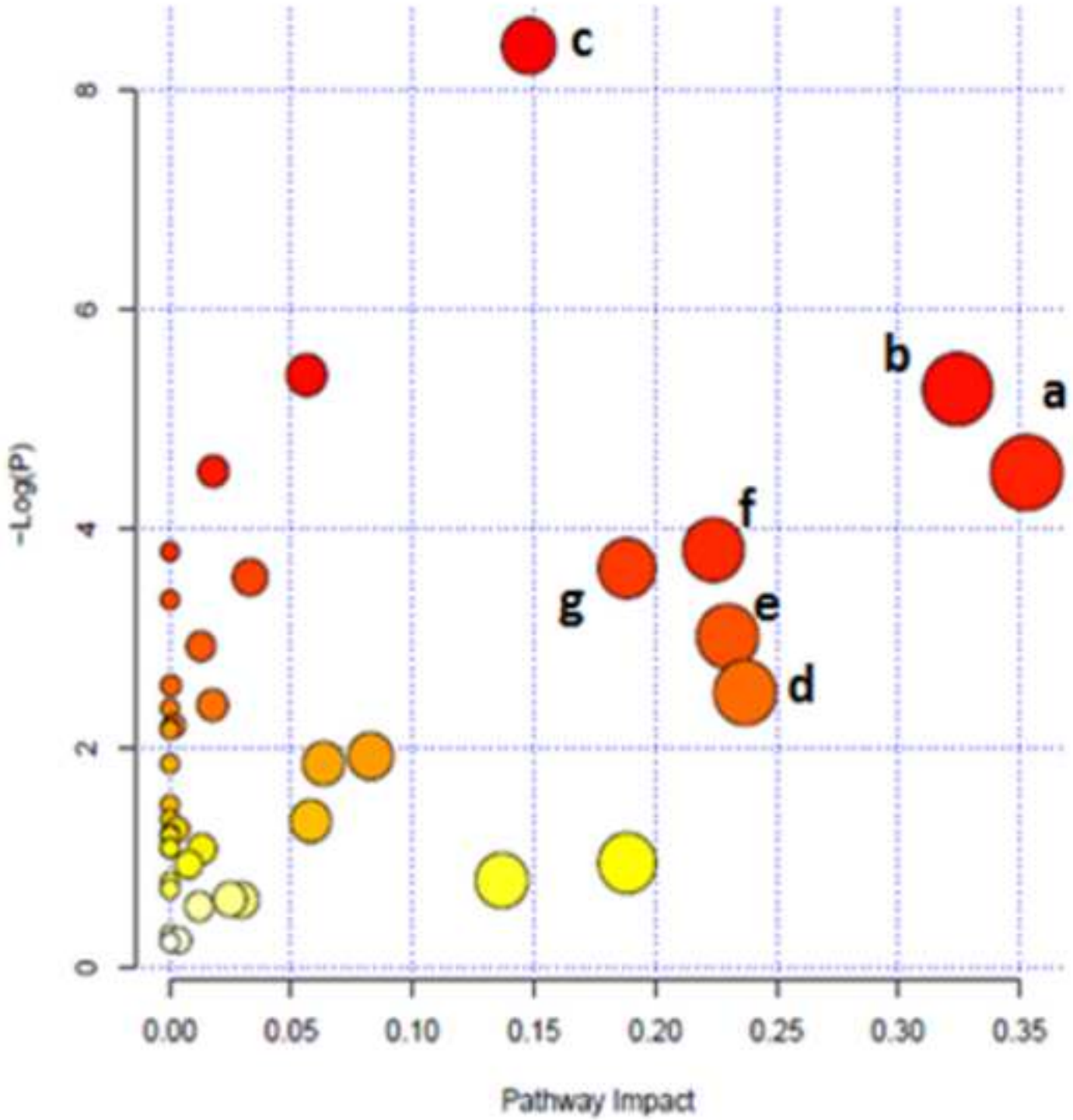

Figure 6

Click here to download high resolution image

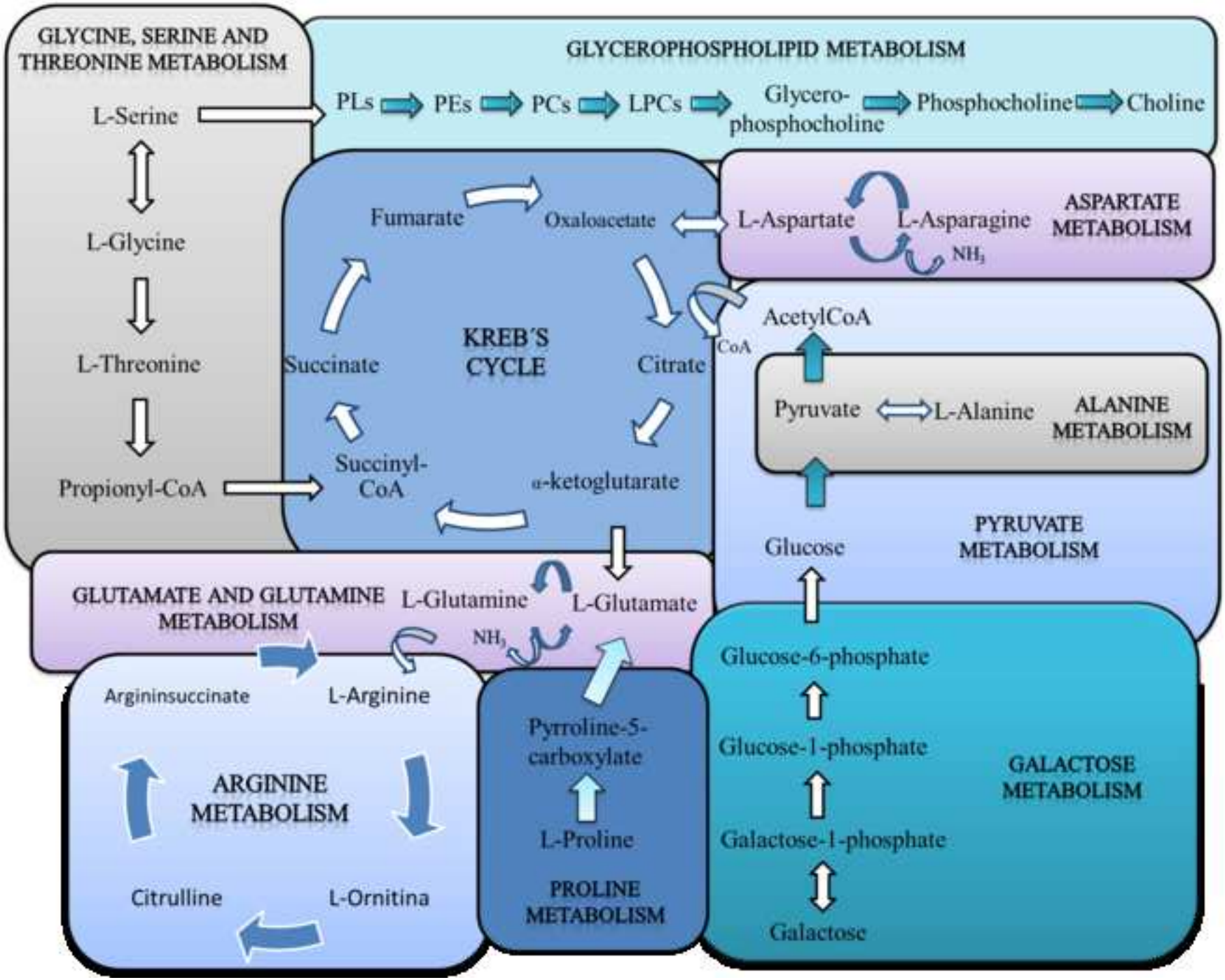

Figure 7

Click here to download high resolution image

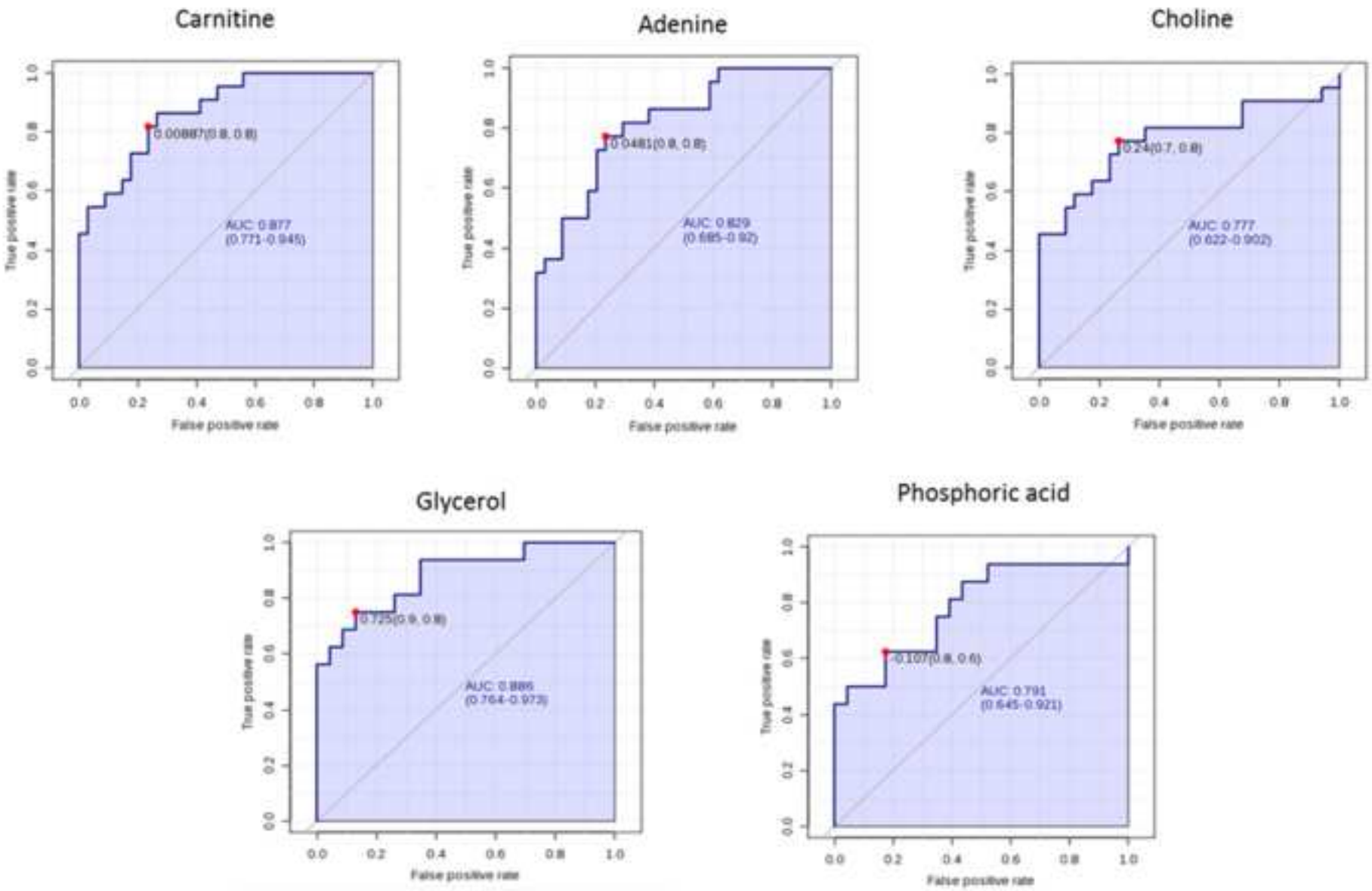

***Conflict of Interest**

Click here to download Conflict of Interest: Conflict of interest.docx